

Absolute Configuration of Bromochlorofluoromethane from Molecular Dynamics Simulation of Its Enantioselective Complexation by Cryptophane-C

Jeanne Costante-Crassous,[†] Tami J. Marrone,[‡] James M. Briggs,[‡]
J. Andrew McCammon,^{*,‡} and André Collet^{*,†}

Contribution from *Stéréochimie et Interactions moléculaires (UMR CNRS 117), École normale supérieure de Lyon, 69364 Lyon cedex 07, France, and Department of Chemistry and Biochemistry and Department of Pharmacology, University of California at San Diego, La Jolla, California 92093-0365*

Received January 15, 1997. Revised Manuscript Received February 21, 1997[⊗]

Abstract: Earlier NMR experiments (Canceill et al. *J. Am. Chem. Soc.* **1985**, *107*, 6993) have shown that the inclusion of bromochlorofluoromethane (CHFCIBr) **1** within the cavity of (–)-cryptophane-C **2** in chloroform solution is enantioselective and that (–)-**1** is more strongly bound than (+)-**1** with a free energy difference ($\Delta\Delta G^\circ_{\text{exp}}$) of 1.1 kJ mol⁻¹. In order to gain information on the relative configuration of the diastereomeric complexes and hence on the absolute configuration of **1**, we have tried to reproduce these experiments by computational methods, and we have calculated the free energy difference for the binding of (*R*) and (*S*)-**1** to (–)-**2**. For this purpose, the OPLS parameters for CHFCIBr were optimized by Monte Carlo (MC) simulations of the pure liquid. Then molecular dynamics (MD) simulations were performed on the host–guest system in a solvent box of chloroform using multiconfiguration thermodynamic integration (MCTI) and free energy perturbation (FEP) methods to calculate the free energy difference between the diastereomeric complexes. The [(*R*)-**1**@(–)-**2**] complex was thus calculated to be more stable than the [(*S*)-**1**@(–)-**2**] one by ($\Delta\Delta G^\circ_{\text{calc}}$) 0–2.6 kJ mol⁻¹, which is of the same order of magnitude as the experimental result. Since the [(–)-**1**@(–)-**2**] complex is more stable than the [(+)-**1**@(–)-**2**] one, and since the absolute configuration of **2** is known, it was concluded that the absolute configuration of CHFCIBr must be (*R*)-(–) (or (*S*)-(+)); this conclusion is in agreement with a recent independent assignment based on Raman Optical Activity studies.

Introduction

Since the first synthesis of bromochlorofluoromethane (CHFCIBr) **1** by Swarts a century ago,¹ a number of attempts² have been made to separate its enantiomers and measure their optical activity. This quest culminated in 1985 when the ¹H NMR analytical resolution of a weakly resolved sample obtained by Wilen³ enabled Canceill et al.⁴ to evaluate its maximum rotation at $[\alpha]^{25}_{\text{D}} \pm 1.6$ (neat, $\rho = 1.91$ kg dm⁻³). A further step was made in 1989 when Doyle and Vogl⁵ reported that partially resolved strychnine salts of bromochlorofluoroacetic acid decarboxylate on heating to give **1** with an amazing conservation of optical activity. Meanwhile, the absolute configuration of CHFCIBr had been the object of speculations,^{6,7} and the recent record⁸ of a good quality Raman Optical Activity (ROA) spectrum of (–)-CHFCIBr (obtained⁹ using Doyle's method) together with relevant calculations which are considered to be quite reliable allowed for the assignment of the (*R*)¹⁰ absolute

configuration to (–)-**1**. This assignment implies that the above mentioned decarboxylation of bromochlorofluoroacetic acid takes place with retention of configuration, a result which seems to be in line with recent observations on the decarboxylation of other α -fluoro carboxylic acids.¹¹

When configurational assignments are discussed, it is always preferable to rely on several arguments, and in order to strengthen the above conclusion we desired to establish the absolute configuration of **1** by a method that would not involve chiroptical properties. In this context, it became interesting to look further into the mechanism of the above mentioned ¹H NMR resolution of **1**, which rests on the enantioselective inclusion of the latter into the chiral cavity of (–)-cryptophane-C **2**, which here acts as a chiral host shift reagent (Figure 1). Apart from certain cyclodextrin-based chiral stationary phases which proved capable of resolving **1** by gas chromatography ($\alpha \approx 1.03$ – 1.06),¹² cryptophane-C is presently the only host known to discriminate efficiently between the enantiomers of this molecule. The relative free energy of binding of the (+)- and

* Correspondence to Prof. André Collet ENS-Lyon, Stéréochimie, 69364 Lyon cedex 05, France. Fax: +33 (0)4 72 72 84 83, e-mail: andre.collet@ens-lyon.fr.

[†] École normale supérieure de Lyon.

[‡] University of California at San Diego.

[⊗] Abstract published in *Advance ACS Abstracts*, April 1, 1997.

(1) Swarts, F. *Bull. Acad. R. Belg.* **1893**, *26*, 102; **1896**, *31*, 28. Swarts, F. *Mémoires couronnés* **1896**, *54*, 1–26.

(2) Berry, K. L.; Sturtevant, J. *J. Am. Chem. Soc.* **1942**, *64*, 1599–1600. Hargreaves, M. K.; Modarai, B. *J. Chem. Soc. C* **1971**, 1013–1015. Hargreaves, M. K.; Modarai, B. *J. Chem. Soc. D* **1969**, 16.

(3) Wilen, S. H.; Bunding, K. A.; Kascheres, C. M.; Wieder, M. J. *J. Am. Chem. Soc.* **1985**, *107*, 6997–6998.

(4) Canceill, J.; Lacombe, L.; Collet, A. *J. Am. Chem. Soc.* **1985**, *107*, 6993–6996.

(5) Doyle, T. R.; Vogl, O. *J. Am. Chem. Soc.* **1989**, *111*, 8510–8511.

(6) Brewster, J. H. *J. Am. Chem. Soc.* **1959**, *81*, 5475–5483.

(7) Applequist, J. *Acc. Chem. Res.* **1977**, *10*, 79–85. See also earlier semiempirical calculations of the vibrational circular dichroism and Raman optical activity spectra based on group or bond polarizabilities: Barron, L. D.; Clark, B. P. *Molec. Phys.* **1982**, *46*, 839–851. Prasad, P. L.; Nafie, L. A. *J. Chem. Phys.* **1979**, *70*, 5582–5588.

(8) Costante, J.; Hecht, L.; Polaravapu, P. L.; Collet, A.; Barron, L. D. *Angew. Chem., Int. Ed. Engl.* **1997**, In press.

(9) Costante, J.; Ehlinger, N.; Perrin, M.; Collet, A. *Enantiomer* **1996**, *1*, 377–386.

(10) The empirical rule of Brewster (ref 6) as well as a sophisticated model used by Applequist (ref 7) also predict **1** to have (*S*)-(+)- or (*R*)-(–) configuration, although these models assume opposite polarizability orders for H vs F.

(11) Schurig, V.; Juza, M.; Green, B. S.; Horakh, J.; Simon, A. *Angew. Chem., Int. Ed. Engl.* **1996**, *35*, 1680–1682.

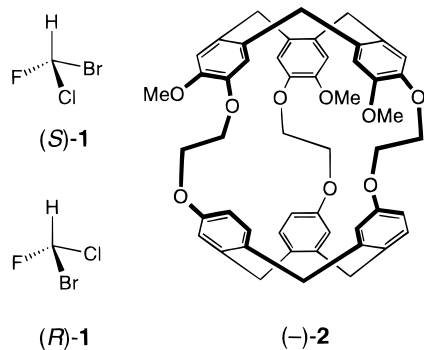


Figure 1. Structures of (*R*)- and (*S*)-CHFCIBr (**1**) and absolute configuration of (–)-cryptophane-C (**2**).

(–)-enantiomers of **1** to (–)-**2** was evaluated to be $(\Delta\Delta G^\circ)_{\text{exp}}$ 1.1 kJ mol^{–1} with a good accuracy ($\pm 5\%$) and almost no variation with temperature in the range 215–332 K, the diastereomeric complex [(–)-**1**@(–)-**2**] being more stable than the [(+)-**1**@(–)-**2**] one. Although the absolute configuration of host **2** is known⁴ (see Figure 1), the relative configurations of the host–guest pairs could not be derived from the NMR data, and it was therefore not possible to establish the absolute configuration of **1** from these experiments. The purpose of the work reported here was to address this problem by means of molecular dynamics (MD) and Monte Carlo (MC) simulations and free energy calculations of the interaction of (*R*) and (*S*)-**1** with (–)-**2** in chloroform. In recent years computational methods and particularly free energy calculations^{13–16} have been increasingly used in supramolecular chemistry^{17,18} as a tool for analyzing molecular recognition processes in the light of statistical thermodynamics. In this context, specific enantioselective recognition problems have recently been addressed by Still^{19,20} (amino acids binding to podand ionophores) and Lipkowitz²¹ (chiral analytes binding to chiral chromatographic surfaces). In these systems however the main driving force for binding is provided by relatively strong polar interactions (hydrogen-bonding) which convey some ordering to the host–guest assemblies, and these forces are not likely to be important in the case we consider here. The question was therefore to assess whether and how the present state-of-the-art simulation techniques can model systems in which the dominant chiral discrimination effects originate from van der Waals forces operating within host–guest complexes that are essentially disordered.

The results presented below show that this goal can indeed be reached. Free energy calculations using multiconfigurational thermodynamic integration (MCTI) and free energy perturbation (FEP) methods actually yielded the correct magnitude of the free energy difference between the diastereomeric complexes,

(12) Grosenick, H.; Schurig, V.; Costante, J.; Collet, A. *Tetrahedron: Asymmetry* **1995**, *6*, 87–88; Beil, A.; Luckhaus, D.; Quack, M. *Ber. Bunsenges Phys. Chem.* **1995**, *100*, 1853–1875.

(13) Straatsma, T. P.; McCammon, J. A. *J. Chem. Phys.* **1991**, *95*, 1175–1188. McCammon, J. A. *Science* **1987**, *238*, 486–491.

(14) Straatsma, T. P.; Zacharias, M.; McCammon, J. A. *Computer Simulation of Biomolecular Systems. Theoretical and Experimental Applications*; ESCOM Science Publishers B. V.: Leiden, 1993; Vol. 2, p 349.

(15) Beveridge, D. L.; DiCapua, F. M. *Annu. Rev. Biophys. Biophys. Chem.* **1989**, *18*, 431–492.

(16) Jorgensen, W. L. *Acc. Chem. Res.* **1989**, *22*, 184–189.

(17) Cannon, W. R.; Madura, J. D.; Thummel, R. P.; McCammon, J. A. *J. Am. Chem. Soc.* **1993**, *115*, 879–884.

(18) Sun, Y.; Kollman, P. A. *J. Am. Chem. Soc.* **1995**, *117*, 3599–3604.

(19) Burger, M. T.; Armstrong, A.; Guarnieri, F.; McDonald, D. Q.; Still, W. C. *J. Am. Chem. Soc.* **1994**, *116*, 3593–3594.

(20) McDonald, D. Q.; Still, W. C. *J. Am. Chem. Soc.* **1996**, *118*, 2073–2077.

(21) Lipkowitz, K. B.; Demeter, D. A.; Zegarra, R.; Larter, R.; Darden, T. *J. Am. Chem. Soc.* **1988**, *110*, 3446–3452.

Table 1. OPLS Parameters for CHFCIBr

site	charge	σ (Å)	ϵ (kJ mol ^{–1})
H	0.102	2.50	0.125
C	0.307	3.60	0.209
Cl	–0.115	3.47	1.112
F	–0.189	2.75	0.339
Br	–0.105	3.65	1.647

and comparison of this result with the NMR experiments led to the conclusion that the absolute configuration of (–)-**1** must be (*R*), in agreement with the ROA experiments.

Computational Details

Given the small difference in the binding free energies of the (+)- and (–)-enantiomers of **1** to host **2** (1.1 kJ mol^{–1}), great care was taken in the development of reliable potential functions parameters for CHFCIBr using MC simulations of the pure liquid.²² Similar care was also taken in choosing the computational conditions for free energy calculations in order to reduce the statistical error associated with MD simulations.

OPLS²³ Parameters Development for CHFCIBr. The intermolecular potential function of a dimer consists of Coulomb and Lennard-Jones interactions between all pairs of sites *a* and *b* on the two monomers (eq 1). Standard combining rules are employed such that $A_{ij} = (A_{ii}A_{jj})^{1/2}$ and $C_{ij} = (C_{ii}C_{jj})^{1/2}$ where $A_{ii} = 4\epsilon_i\sigma_i^6$ and $C_{ii} = 4\epsilon_i\sigma_i^6$ in terms of Lennard-Jones σ 's and ϵ 's.

$$\Delta E_{ab} = \sum_i \sum_j^{on.aon.b} \left(\frac{q_i q_j e^2}{r_{ij}} + \frac{A_{ij}}{r_{ij}^{12}} - \frac{C_{ij}}{r_{ij}^6} \right) \quad (1)$$

The optimized geometry and the energy of **1** were obtained by Quantum Mechanics (QM) calculations at the Hartree–Fock level using the GAUSSIAN 94 program²⁴ and the 6-311+G* basis set (6-311+G* // 6-311+G*). Atomic centered charges were obtained from an electrostatic potential fit to the wave functions using the CHELPG²⁵ method. These charges (see Table 1) were used throughout the remaining calculations. Then standard Monte Carlo (MC) simulations (including Metropolis sampling and the isothermal-isobaric NPT ensemble)²⁶ were performed on the pure liquid CHFCIBr using the BOSS v3.6 program.²⁷ A box of 289 molecules of (*R*)-CHFCIBr was equilibrated for 3×10^6 configurations, and the density $\rho = 289M/N_aV$ and heat of vaporization $\Delta H_v = -E_{\text{tot}}/289 + RT$ were computed at 300 K from a statistical averaging over these configurations. The optimized parameters assembled in Table 1 were then obtained by fitting the density and the enthalpy of vaporization to the experimental values. The final computed value of ρ was 1.90 g cm^{–3} (exp 1.91)^{1,4} and that of ΔH_v was 26.2 kJ mol^{–1}, which is close to the value calculated from Trouton's rule (26.4 kJ mol^{–1}).

Gas-Phase Studies. In order to get further information about Lennard-Jones parameters, the interactions between the hydro-

(22) Briggs, J. M.; Nguyen, T. B.; Jorgensen, W. L. *J. Phys. Chem.* **1991**, *95*, 3315–3322.

(23) Optimized Potentials for Liquids Simulations. Jorgensen, W. L.; Tirado-Rives, J. *J. Am. Chem. Soc.* **1988**, *110*, 1657–1666.

(24) Frisch, M. J.; Head-Gordon, M.; Trucks, G. W.; Foresman, J. B.; Schlegel, H. B.; Raghavachari, K.; Robb, M. A.; Binkley, J. S.; Gonzalez, C.; Defrees, D. J.; Fox, D. J.; Whiteside, R. A.; Seeger, R.; Melius, C. F.; Baker, J.; Martin, R. L.; Kahn, L. R.; Stewart, J. J. P.; Topiol, S.; Pople, J. A. *GAUSSIAN 94*; Gaussian, Inc.: Pittsburgh, PA, 1994.

(25) Breneman, C. M.; Wiberg, K. B. *J. Comput. Chem.* **1990**, *11*, 361–373.

(26) Allen, M. P.; Tildesley, D. J. *Computer Simulations of Liquids*; Oxford University Press: Oxford, 1987.

(27) Jorgensen, W. L. *BOSS 3.6*: New Haven, 1995.

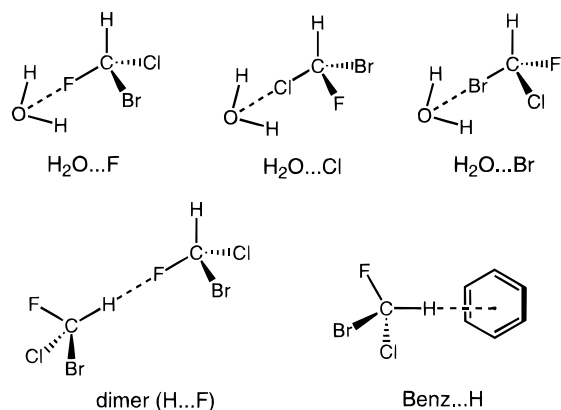


Figure 2. Complexes whose intermolecular distances have been optimized in the gas phase using quantum mechanics and OPLS force field calculations.

Table 2. Optimized Intermolecular Distances and Interaction Energies ΔE for Each Complex Studied in the Gas Phase Using Either QM or OPLS Force Field Calculations

complex	intermolecular distance (Å)	ΔE (kJ mol ⁻¹)	method
H ₂ O...F	3.14	-5.98	QM
H ₂ O...F	2.94	-4.97	OPLS
H ₂ O...Cl	4.62	+0.04	QM
H ₂ O...Br	6.89	+0.64	QM
dimer (H...F)	2.50	-3.93	QM
dimer (H...F)	2.48	-5.10	OPLS
Benz...H	2.81	-9.24	QM
Benz...H	2.56	-15.88	OPLS

gen or one of the three halogens of CHFCIBr with different molecules such as H₂O, benzene, or another CHFCIBr (Figure 2) were studied in the gas phase. The distance *vs* interaction energy was optimized either by means of QM with the 6-311+G* basis set using the GAUSSIAN 94 program or by molecular mechanics (MM) using the OPLS force field. Because these methods are not equivalent (the present MM calculations do not allow bond length variations), in both cases the intramolecular geometries were held fixed in their OPLS form (CHFCIBr-this work, HOH-TIP4P,²⁸ benzene²⁹). The results of these calculations are summarized in Table 2.

Molecular Dynamics. Molecular dynamics (MD) of the empty (-)cryptophane-C and of the host containing one chloroform molecule were then performed in a chloroform solvent box using ARGOS 6.1³⁰ in the NPT ensemble. An all atom representation was employed for this study. Internal bonded and nonbonded parameters were obtained from previous work by Kirchhoff *et al.* on a different cryptophane (after applying appropriate scaling factors).³¹ These parameters are mainly the OPLS-AMBER ones and are summarized in Table 3 and in Kirchhoff's paper. The atomic centered charges were obtained from an electrostatic potential fit to the wave functions using the CHELPG²⁵ method on three different monomers, namely 3,4-dimethylanisole, 3,4-dimethylveratrole, and ethyleneglycol in their OPLS form, using the 6-311G* basis sets (Figure 3). These atomic charges were subsequently rearranged in order to obtain a neutral cryptophane-C (see Table 3).

(28) Jorgensen, W. L.; Chandrasekhar, J.; Madura, J. D.; Impey, R. W.; Klein, M. L. *J. Chem. Phys.* **1983**, *79*, 926.

(29) Jorgensen, W. L.; Laird, E. R.; Nguyen, T. B.; Tirado-Rives, J. *J. Comput. Chem.* **1993**, *14*, 206-215. Jorgensen, W. L.; Nguyen, T. B. *J. Comput. Chem.* **1993**, *14*, 195-205.

(30) Straatsma, T. P.; McCammon, J. A. *J. Comput. Chem.* **1990**, *11*, 943-951.

(31) Kirchhoff, P. D.; Bass, M. B.; Hanks B. A.; Briggs, J. M.; Collet, A.; McCammon, J. A. *J. Am. Chem. Soc.* **1996**, *118*, 3237-3246.

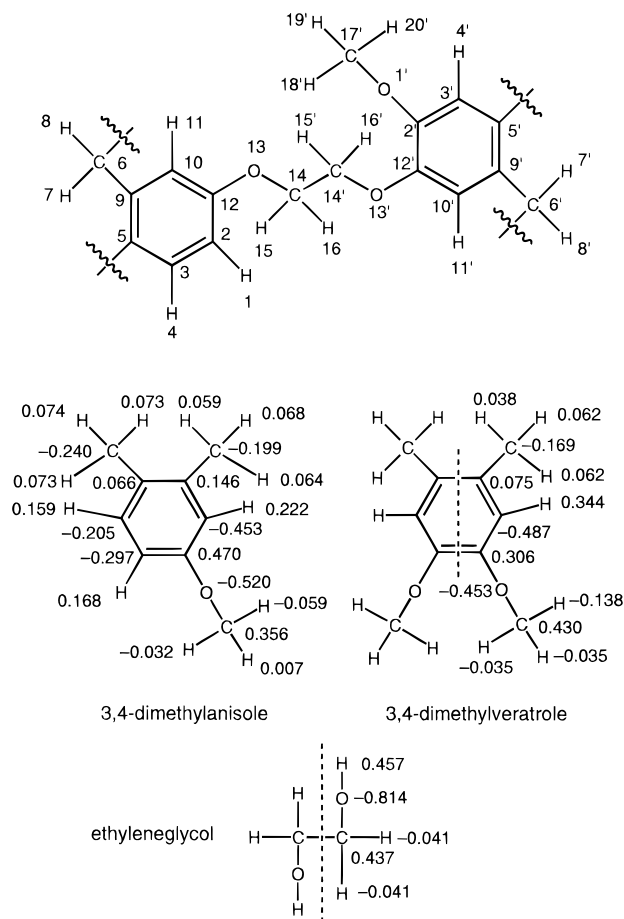


Figure 3. Atom numbering used for cryptophane-C and atom-centered charges obtained using the CHELPG method.

Table 3. Charges and Lennard-Jones Parameters Used for Cryptophane-C

OPLS atom type	Q (atomic charges)	σ (Å)	ϵ (kJ mol ⁻¹)	atom no. (Figure 3)
231HC	0.168	2.42	0.125	1, 4
230CA	-0.297	3.55	0.293	2
230CA	-0.205	3.55	0.293	3
230CA	0.066	3.55	0.293	5
291CT	-0.410	3.50	0.276	6
295HC	0.145	2.50	0.125	7, 8
230CA	0.146	3.55	0.293	9
230CA	-0.453	3.55	0.293	10
231HC	0.222	2.42	0.125	11
230CA	0.470	3.55	0.293	12
302OS	-0.520	3.00	0.170	13
291CT	0.360	3.50	0.276	14
295HC	-0.041	2.50	0.125	15, 16
302OS	-0.453	3.00	0.170	1', 13'
230CA	0.306	3.55	0.293	2', 12'
230CA	-0.464	3.55	0.293	3'
231HC	0.253	2.42	0.125	4'
230CA	0.075	3.55	0.293	5', 9'
291CT	-0.410	3.50	0.276	6'
295HC	0.145	2.50	0.125	7', 8'
230CA	-0.487	3.55	0.293	10'
231HC	0.344	2.42	0.125	11'
291CT	0.437	3.50	0.276	14'
295HC	-0.041	2.50	0.125	15', 16'
291CT	0.430	3.50	0.276	17'
295HC	-0.030	2.50	0.125	18', 19', 20'

Because no chloroform solvent box was available in the ARGOS 6.1 package, the box was created using MC simulations by performing 10×10^6 configurations of equilibration on the empty host in chloroform. The resulting cubic box consisted

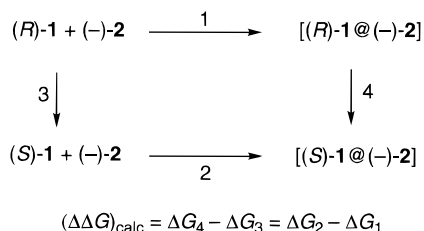


Figure 4. Thermodynamic cycle used for free energy calculations.

of 435 chloroform molecules with dimensions of 39*39*39 Å³. The starting coordinates used for (–)-cryptophane-C were those of the crystal structure of the [CH₂Cl₂@(±)-2] complex.³² Then typical equilibration steps in the MD simulations were performed using periodic boundary conditions. First, the solvent energy was relaxed using steepest descent minimization while the solute was held fixed. Second, MD was conducted on the solvent at 300 K for 20 ps with velocity reassignment every 0.2 ps, while the solute was held fixed. Third, energy minimization using steepest descent steps and then MD was conducted on the solute for 5 ps intervals at temperatures 100, 200, and 300 K with velocity reassignment every 0.2 ps, while the solvent was held fixed. Finally, MD was conducted on the entire system at 300 K for 10 ps with velocity reassignment every 0.5 ps followed by 20 ps simulation with no velocity reassignment. During the simulation, the short range cutoff was 9 Å, and the long range cutoff was 14 Å for solvent–solvent, solvent–solute, and solute–solute interactions. SHAKE³³ was used to fix all bond lengths to their equilibrium values.

Free Energy Calculations. The major theoretical tool for MD and MC³⁴ studies of host–guest complexes is the thermodynamic cycle-perturbation method^{35,36} (Figure 4). In this cycle the experimentally measured parameter ($\Delta\Delta G^\circ$)_{exp} corresponds to ($\Delta G_2 - \Delta G_1$), which is also equal to ($\Delta G_4 - \Delta G_3$). Instead of calculating separately the free energy of binding related to processes 1 (ΔG_1) and 2 (ΔG_2) which would eventually give ($\Delta\Delta G^\circ$)_{calc} as a small difference of two large numbers, it is much more accurate to study the mutation of (R)-CHFCIBr into (S)-CHFCIBr (stepwise conversion of Br into Cl and vice-versa) inside of the cryptophane cavity (process 4) and alone (process 3), in chloroform. This process which gives access to ($\Delta\Delta G^\circ$)_{calc} as the difference $\Delta G_4 - \Delta G_3$ has the advantage that ΔG_3 , which is normally equal to zero, provides a good test of the reliability of the calculation, and ΔG_4 is thus almost exactly the desired ($\Delta\Delta G^\circ$)_{calc}. These relative free energy differences were evaluated using MD and the MCTI and FEP methods with a control variable λ describing the mutation. First the system was equilibrated by doing all the molecular dynamics steps described above, and then MCTI and FEP were performed at 300 K using 21 λ steps, 3000 configurations for equilibration, and 5000 configurations for sampling each λ step. In the MCTI method the free energy difference between initial and final states is then given by eq (2)

$$\Delta G = \sum_i \left\langle \frac{\partial H}{\partial \lambda} \right\rangle_{\lambda_i} \Delta \lambda_i \quad (2)$$

(32) Canceill, J.; Cesario, M.; Collet, A.; Guilhem, J.; Pascard, C. *J. Chem. Soc., Chem. Commun.* **1985**, 361–363.

(33) Ryckaert, J.-P.; Ciccotti, G. and Berendsen, H. J. C. *J. Comp. Phys.* **1977**, 23, 327.

(34) See ref 26 and McCammon, J. A.; Harvey, S. C. *Dynamics of Proteins and Nucleic Acids*; Cambridge University Press: New York, 1987.

(35) Straatsma, T. P.; McCammon, J. A. *Annu. Rev. Phys. Chem.* **1992**, 43, 407–435.

(36) Cannon, W. R.; Briggs, J. M.; Shen, J.; McCammon, J. A.; Quirocho, F. A. *Protein Science* **1995**, 4, 387–393.

where H is the Hamiltonian, which depends on λ , and i counts over the number of different values of λ ; $\Delta\lambda_i$ is the difference between successive values of λ . An ensemble average is generated for each value of λ by MD. In the FEP method $\Delta G = \sum_i \Delta G_i$ is evaluated by means of eq (3),

$$\Delta G_i = kT \ln \left\langle \exp \left\{ - \frac{H_{i-1/2} - H_i}{kT} \right\} \right\rangle_{\lambda_i} - kT \ln \left\langle \exp \left\{ - \frac{H_{i+1/2} - H_i}{kT} \right\} \right\rangle_{\lambda_i} \quad (3)$$

where k is the Boltzmann's constant, T the absolute temperature $H_i = H(\lambda_i)$, $H_{i-1/2} = H(\lambda_i - (1/2)\{\lambda_i - \lambda_{i-1}\})$, and $H_{i+1/2} = H(\lambda_i + (1/2)\{\lambda_i - \lambda_{i-1}\})$. The ensemble average is generated for each value of λ_i by MD.

Results and Discussion

Our major concern in this study was the accuracy of the potential energy function used to describe the binding process in order to account for such a small free energy difference as 1.1 kJ.mol⁻¹. As was said above the OPLS parameter development for pure liquid CHFCIBr allowed us to reproduce the experimental density ρ and heat of vaporization ΔH_v of this haloform very well. In the gas-phase study, the high-level QM calculations and the OPLS force field calculations were in agreement not only for the intermolecular distances but also for the interaction energies ΔE (Table 2). These calculations revealed a weak attractive interaction (*ca.* –5 kJ mol⁻¹ at 2.5 Å separation) between H and F in the CHFCIBr dimer, a result which is not particularly surprising in view of the electronegativity of F. The interaction between CHFCIBr and benzene was also quantified because cryptophane-C has six aromatic rings. We actually found a moderately attractive interaction (–9.2 to –15.9 kJ mol⁻¹) between the haloform C–H and a benzene ring held perpendicular to this bond at a H•••benzene distance of *ca.* 2.7 Å. These figures are in line with recent MC simulations by Jorgensen et al.³⁷ of the Cl₃CH–benzene interaction (with a 4-site model used for chloroform) and which suggested an interaction energy of –16.3 kJ mol⁻¹ at a C•••benzene separation of 3.4 Å. In view of these results, the OPLS parameters we obtained for CHFCIBr were consistent enough to be used for the potential functions to describe systems consisting of one molecule of **1** inside the cryptophane **2** in chloroform as the solvent.

We now turn to the simulations performed on (–)-cryptophane-C itself and on its complexes. The structure of this cryptophane consists of two [1.1.1]orthocyclophane caps linked to one another by three OCH₂CH₂O spacer bridges. The upper cap in Figure 1 bears three OMe groups at its periphery, ortho to the spacer bridges. These OMe groups are not present on the lower cap. In an idealized geometry this cryptophane displays a North–South 3-fold axis and belongs to the C₃ point group. The North and South regions are mostly aromatic in nature, the upper and lower tropical belts contain six and three oxygen atoms, respectively, and the equatorial region contains the three CH₂CH₂ fragments. The three pores giving access to the cavity are located in this region, and the three OMe groups do not seem to obstruct these pores very efficiently. In fact host **2** complexes guests of the size of **1** or of chloroform reversibly, with a barrier to entrance and departure in the range of 50–60 kJ mol⁻¹.³⁸ Molecular dynamics provided interesting

(37) Jorgensen, W. L.; Severance, D. L. *J. Am. Chem. Soc.* **1990**, 112, 4768–4774.

(38) Collet, A. *Cryptophanes*. In *Comprehensive Supramolecular Chemistry*; Vögtle, F., Ed.; Pergamon: 1996; Vol. 2, Chapter 11, pp 325–365.

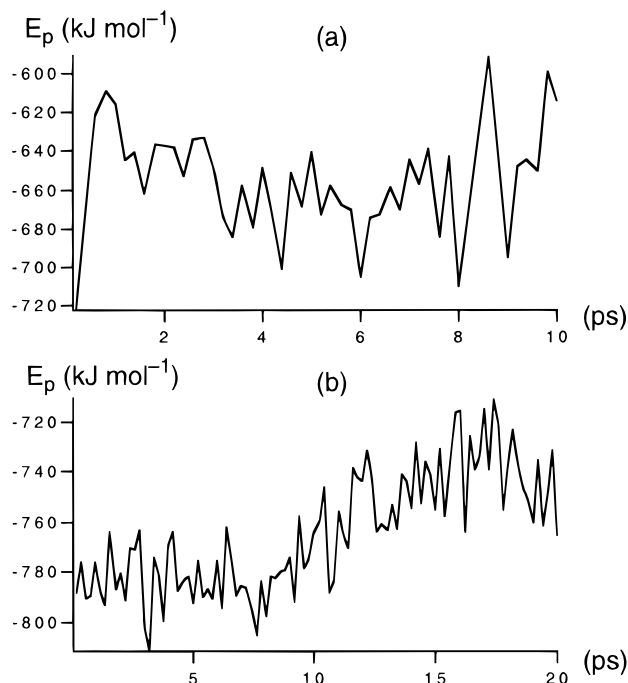


Figure 5. Plot of the potential energy of the empty cryptophane-C during the last two steps of the MD equilibration: (a) entire system at 300 K for 10 ps with velocity reassignment and (b) no velocity reassignment.

insight into the degree of conformational flexibility of cryptophane-C and its behavior in the absence and in the presence of a guest molecule. When MD was performed on an empty cryptophane in chloroform, the molecule became strongly distorted from its ideal 3-fold symmetry and the total potential energy, instead of being constant, proved to increase with time (Figure 5). The dynamic fluctuations were observed using QUANTA³⁹ and revealed that the OMe groups were trying to penetrate into the empty host cavity. When MD was performed on a cryptophane containing one chloroform molecule inside, in chloroform, the new system proved to be much more stable, the total potential energy remained constant during the MD simulation (Figure 6). For the duration of the simulation, the C–H bonds of CHCl₃ remained oriented roughly parallel to the North–South axis of the host. When MD was performed with one of the C–halogen bond of the guest directed along the North–South axis at the beginning of the simulation, the guest rapidly reoriented itself in order to have its C–H bond eventually aligned with the host axis and the three halogens in the equatorial region. The same behavior was found with CHFClBr as the guest, and this feature was taken into account in the free energy calculations discussed below.

We next performed the mutation of (*R*) to (*S*)-CHFClBr in chloroform in order to compute the free energy change ΔG_3 of process 3 (Figure 4) which, as said above, should be equal to zero. In this way, ΔG_3 was calculated to be -0.14 ± 1.12 kJ mol⁻¹ by MCTI and -0.14 ± 0.66 kJ mol⁻¹ by FEP. These figures are quite consistent and reasonably close to zero, with the statistical error being, however, of the same order of magnitude as $(\Delta\Delta G^\circ)_{\text{exp}}$.

In order to perform the mutation of (*R*) to (*S*)-CHFClBr within the complex (process 4), it is necessary to define the orientation of the guest with respect to the North–South 3-fold axis of the host at the onset of the MD simulation. As said above, the conformations where one of the C–halogen bond is directed

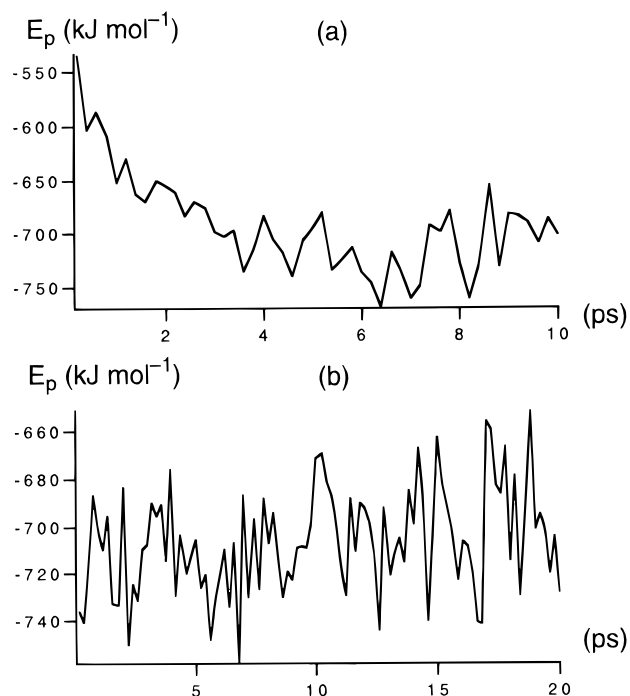


Figure 6. Plot of the potential energy of cryptophane-C occupied with one chloroform molecule during the last two steps of the MD equilibration: (a) entire system at 300 K for 10 ps with velocity reassignment and (b) no velocity reassignment.

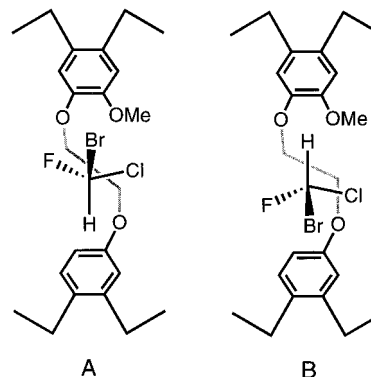


Figure 7. Orientations of the guest C–H bond used for the free energy calculations.

along the 3-fold axis of the host being much higher in energy than those where the C–H bond is oriented in this way are eliminated during the equilibration. Accordingly there remain only two different situations to consider, differing by the orientation of the guest C–H bond which can be either turned toward the lower cap (A) or towards the upper cap (B) of the host (see Figure 7). These two cases which are very close in energy were used in the MD study, and no transition between them or to a different state were observed during the 5000 steps of each equilibration. This is in line with the observations that in the two crystal structures of cryptophane-CHCl₃ complexes that have been solved the C–H bond is aligned with the 3-fold axis of the host and the three halogens reside in the equatorial plane.⁴⁰ Despite the fact that the statistical error was again of the same order of magnitude as the considered free energy change, the MCTI and FEP calculations provided consistent values for ΔG_4 , namely 1.40 ± 1.19 kJ mol⁻¹ (MCTI) and 1.37 ± 0.65 kJ mol⁻¹ (FEP).

(39) Biosym Technologies/Molecular Simulations Inc. 1994, 9685 Scranton Road, San Diego, CA 92121-4778.

(40) Canceill, J.; Cesario, M.; Collet, A.; Guilhem, J.; Lacombe, L.; Lozach, B.; Pascard, C. *Angew. Chem., Int. Ed. Engl.* **1989**, *28*, 1246–1248. Garcia, C.; Antoine, C.; Perrin, M.; Collet, A. To be published.

The complex [(R)-**1**@(-)-**2**] is thus calculated by this method to be more stable than its diastereomer [(S)-**1**@(-)-**2**] by $(\Delta\Delta G^\circ)_{\text{calc}} 0-2.6 \text{ kJ mol}^{-1}$ if the statistical error is considered. This result is incredibly close to the $(\Delta\Delta G^\circ)_{\text{exp}}$ and, as such, leaves little doubt as to the relative stereochemistry of the two complexes. Since the NMR experiments indicate that the complex [(-)-**1**@(-)-**2**] is the most stable, the present calculations in turn lead to assignment of the (*R*) configuration to (-)-CHFCIBr, which is consistent with the above mentioned ROA determination of the absolute configuration of this haloform. It is worth noting that even though these simulations apparently yield the correct answer—both qualitatively and quantitatively—in terms of free energy difference between a pair of diastereomeric

complexes, they do not furnish information about the structural origin of this difference, and they also suggest that this question has little relevance in such disordered systems where a great number of states of comparable energy contribute to the generation of a weak discrimination.

Acknowledgment. We are grateful to NATO for a grant to JCC (No. 950763) and to the NSF and the NSF supercomputer centers metacenter program for grants. Gratitude is also expressed to Molecular Simulations, Inc., San Diego, CA for providing Quanta and related modules (J.A.M.).

JA9701164